Letters

Efficiency Analysis and Optimization Method of Power-Relay IPT Systems for Reefer Containers

Huanyu Yang, Yefei Xu, Yundong Gu, Chenyan Zhu, Jie Yu, Ruikun Mai, *Senior Member, IEEE*, Yong Li, *Member, IEEE*, Zhengyou He, *Senior Member, IEEE*, and Udaya Kumara Madawala, *Fellow, IEEE*

***Abstract*—In order to get rid of plug-in/out actions for container terminals and to save space, a power-relay inductive power transfer system is employed for reefer container wireless charging. Besides, a load-power-based efficiency model is proposed to analyze system efficiency. The function of efficiency against the input voltage and the load power distributions of the system is analyzed in detail. Then, system efficiency can be improved by regulating the input voltage according to the input-voltage-lookup table, which is generated as per various power distributions of loads. Finally, a prototype with three loads is built to validate the performance of the proposed approach. The experimental results show that the efficiency is greater than 94.29% with an improvement by 7.6%, 7.2%, and 6.0%, compared with those without optimization (fixed input voltage 213 V) at one load (@80 W), two loads (@80 and 80 W), and three loads (@80, 80, and 80 W), respectively.**

***Index Terms*—Efficiency optimization, inductive power transfer (IPT) system, power-relay, reefer container.**

I. Introduction

REEFER containers play an essential role in the cold-chain transportation industry. Nowadays, the reefer containers are powered by the plug-in/out-based power supply systems, which suffer three main drawbacks. First, the physical plug-in connection is labor-intensive and time-consuming, and plugs are prone to fall off undesirably when containers are moved, leading to equipment damage. Second, such systems are not suitable for operating under adverse weather conditions, such as rain, snow, etc. Third, power towers are required to mount power supply systems, as shown in Fig. 1(a), which occupy plenty of space while land resources at container terminals are limited and expensive. Inductive power transfer (IPT) technology can alleviate these drawbacks. IPT facilitates electrical power transfer over an air gap through magnetic coupling without any direct electrical connections and has been employed in many industrial applications, such as automatic guided vehicles (AGV) [1], electrical vehicles [2], [3], etc. Thus, IPT technology is a promising candidate for reefer container charging. The number of reefer containers exceeds 1300 in a large-scale container terminal, and these reefer containers consume 65–195 MWh electrical power per day. Thus, for the IPT systems of reefer containers, system efficiency is one of the critical performances, as it affects the economic benefit significantly.

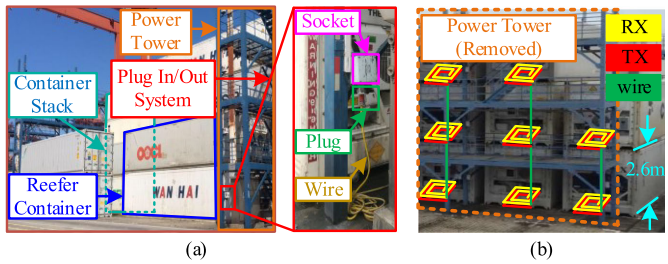

Fig. 1. Reefer container stacks. (a) Reefer containers and power towers. (b) Power-relay IPT system installation diagram.

Recently, lots of efforts have been taken to improve the efficiency of the traditional single-transmitter-and-single-receiver-based IPT systems (1-to-1 systems). The efficiency is dramatically improved by: 1) optimizing system parameters and topologies [4], [5] and 2) using maximum efficiency point tracking (MEPT) control schemes [6], [7]. Moreover, IPT systems with one transmitter and multiple receivers (1-to-*N* systems) have also been investigated. In such systems, multiple receivers can be powered simultaneously. The efficiency optimization of 1-to-*N* systems can be realized by: 1) setting load resistances to the optimal values [8]; 2) tuning the system operating frequency [9], [10]; and 3) regulating the system input voltage [11]–[13].

Unfortunately, for reefer container applications, these 1-to-1 or 1-to-*N* systems require power towers to mount transmitters.

Manuscript received August 21, 2020; revised September 24, 2020; accepted October 4, 2020. Date of publication October 14, 2020; date of current version January 22, 2021. This work was supported in part by the National Natural Science Foundation of China under Grants 51677155, 51977184, and 51907169, in part by the Sichuan Youth Science and Technology Innovation Research Team under Grant 2020JDT0004, in part by the Sichuan Science and Technology Program under Grant 2020YFH0031, and in part by the Fundamental Research Funds for the Central Universities under Grant 2682020CX16. *(Corresponding author: Ruikun Mai.)*

Huanyu Yang, Yefei Xu, Yundong Gu, Chenyan Zhu, Jie Yu, Ruikun Mai, Yong Li, and Zhengyou He are with the Key Laboratory of Magnetic Suspension Technology and Maglev Vehicle, Ministry of Education, Southwest Jiaotong University, Chengdu 611756, China (e-mail: 983911020@qq.com; xuyefei1991@foxmail.com; 986663689@qq.com; zcy@my.swjtu.edu.cn; yujie1315@126.com; mairk@swjtu.edu.cn; leeo1864@163.com; hezy@home.swjtu.edu.cn).

Udaya Kumara Madawala is with The University of Auckland, Auckland 1142, New Zealand (e-mail: u.madawala@auckland.ac.nz).

Color versions of one or more of the figures in this article are available online at https://ieeexplore.ieee.org.

Digital Object Identifier 10.1109/TPEL.2020.3030902

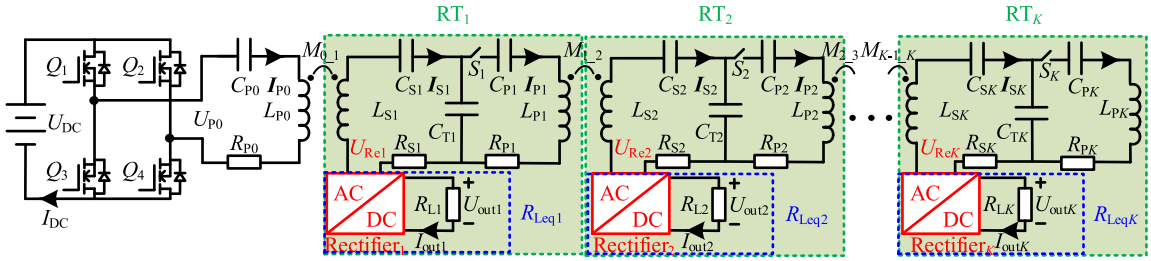

Fig. 2. Power-relay IPT system.

TABLE I
POWER DEMAND OF A TYPICAL REEFER CONTAINER

Working status	Power requirement
refrigeration	6.6kW
heating	3.0kW
air recirculation	1.6kW

About 10.26% of valuable space is occupied by a power tower for a fleet of containers, which increases the land cost.

The power-relay systems might be an alternative solution for powering containers because such systems deliver power one by one without power towers, as shown in Fig. 1(b). The power-relay IPT systems are previously well studied by Zhang *et al.* and Mi *et al.* A power-relay system with equal power distribution and its efficiency optimization method are proposed when all the loads are equal in [14]. However, the optimization method will be unavailable when the loads are not equal. In [15], a power-relay system with equal power distribution is proposed by designing the load to meet a specific condition. Whereas, the output power of other loads will alter with the change of one load. To achieve the independent load power distribution, the power-relay systems with series–parallel–series and *LCC* compensation are proposed in [16] and [17], which make the equivalent loads able to be regulated by dc/dc converters. Those power-relay IPT systems are considered for low-power applications, such as the driver circuits of the power electronics switches, without considering optimal system efficiency. Nevertheless, for the reefer containers applications, system efficiency is one of the most important performances that should be carefully considered. Meanwhile, the power demand of a reefer container usually varies among a few discrete power points according to the work status, as listed in Table I. In a container stack, the containers may work in different states, which affects the system efficiency dramatically. Therefore, it is essential to optimize the efficiency of power-relay IPT systems with various power distributions for reefer containers.

In this letter, the load-power-based efficiency model (LPB-EM) is introduced to illustrate the power-relay IPT system, and a corresponding efficiency optimization method based on input-voltage-lookup tables generated off-line is proposed. The main contributions of this letter are listed as follows.

1) The power-relay systems are applied to power containers, and the systems can be installed on containers without power towers, which can save about 10.26% of valuable space from 212.2 to 190.4 m^2 for a fleet of containers.
2) System efficiency can be improved by regulating the input voltage according to the input-voltage-lookup tables, which are generated as per various power distributions of loads.

II. TOPOLOGY ANALYSIS

A. System Configuration

The power-relay IPT system, as shown in Fig. 2, mainly consists of a dc voltage source, an inverter, a transmitter TX_0, and repeaters $RT_1, RT_2, \ldots, RT_K$ (K is the total number of loads in the IPT system). TX_0 consists of a transmitter coil L_{P0} and a compensation capacitor C_{P0}. Each RT_i ($0<i\leq K$) contains a receiver coil L_{Si}, a transmitter coil L_{Pi}, a rectifier, a load R_{Li}, a switch S_i, and three compensation capacitors C_{Si}, C_{Ti}, and C_{Pi}. M_{i_i+1} denotes the mutual inductance between L_{Pi} and $L_{S(i+1)}$. R_{Leqi} is the equivalent ac load resistor of the combination of the rectifier and R_{Li}. All the cross coupling can be ignored since the distance between L_{Pi} and $L_{P(i+1)}$ is 2.6 m, as shown in Fig. 1(b).

The system is designed to be resonant at the operating angular frequency ω

$$\omega = \frac{1}{\sqrt{L_{P0}C_{P0}}} = \frac{1}{\sqrt{L_{Pi}C_{Pi}C_{Ti}/(C_{Pi}+C_{Ti})}} = \frac{1}{\sqrt{L_{Si}C_{Si}C_{Ti}/(C_{Si}+C_{Si})}}. \quad (1)$$

It is worthy of mentioning that when there are only n ($0<n\leq K$) loads, $RT_{n+1}, \ldots, RT_k$ are removed, and S_n should be OFF to avoid unnecessary power loss in L_{Pn}.

B. Circuit Modeling

The first harmonic approximation is employed to analyze the power-relay IPT system. R_{Pi} and R_{Si} are the equivalent series resistors (ESRs) of L_{Pi} and L_{Si}, respectively. Compared with R_{Pi} and R_{Si}, the ESRs of inductances C_{Si}, C_{Ti}, and C_{Pi} are sufficiently small. Thus, their influence on the system can be neglected. Assuming all the coils are designed as the same despite the tolerance, $M_{i\_i+1}=M$, $R_{Pi}=R_{Si}=r$, and $C_{Ti}=C_T$.

According to Kirchhoff's voltage law (KVL), the system can be described as

$$\begin{bmatrix} \mathbf{U}_{\mathrm{P0}} \\ 0 \\ 0 \\ 0 \\ \dots \\ 0 \end{bmatrix} = \begin{bmatrix} Z_{\mathrm{P0}} & \mathrm{j}\omega M & 0 & 0 & \dots & 0 \\ \mathrm{j}\omega M & Z_{S1} & \frac{1}{\mathrm{j}\omega C_{\mathrm{T}}} & 0 & \dots & 0 \\ 0 & \frac{1}{\mathrm{j}\omega C_{\mathrm{T}}} & Z_{\mathrm{P1}} & \mathrm{j}\omega M & \dots & 0 \\ 0 & 0 & \mathrm{j}\omega M & Z_{\mathrm{S2}} & \dots & 0 \\ \dots & \dots & \dots & \dots & \dots & \dots \\ 0 & 0 & 0 & 0 & \dots & Z_{\mathrm{S}n} \end{bmatrix} \cdot \begin{bmatrix} \boldsymbol{I}_{\mathrm{P0}} \\ -\boldsymbol{I}_{\mathrm{S1}} \\ \boldsymbol{I}_{\mathrm{P1}} \\ -\boldsymbol{I}_{\mathrm{S2}} \\ \dots \\ -\boldsymbol{I}_{\mathrm{S}n} \end{bmatrix} + \begin{bmatrix} 0 \\ \mathrm{j}2\alpha V_{\mathrm{F}} \\ 0 \\ \mathrm{j}2\alpha V_{\mathrm{F}} \\ \dots \\ \mathrm{j}2\alpha V_{\mathrm{F}} \end{bmatrix} \tag{2}$$

where

$$Z_{\mathrm{P0}} = \mathrm{j}\omega L_{\mathrm{P0}} + 1/(\mathrm{j}\omega C_{\mathrm{P0}}) + 2R_{\mathrm{DS}} + r$$
$$Z_{\mathrm{S1}} = \mathrm{j}\omega L_{\mathrm{S1}} + 1/(\mathrm{j}\omega C_{\mathrm{S1}}) + 1/(\mathrm{j}\omega C_{\mathrm{T}}) + R_{\mathrm{Leq1}} + r$$
$$Z_{\mathrm{P1}} = \mathrm{j}\omega L_{\mathrm{P1}} + 1/(\mathrm{j}\omega C_{\mathrm{P1}}) + 1/(\mathrm{j}\omega C_{\mathrm{T}}) + r$$
$$Z_{\mathrm{S2}} = \mathrm{j}\omega L_{\mathrm{S2}} + 1/(\mathrm{j}\omega C_{\mathrm{S2}}) + 1/(\mathrm{j}\omega C_{\mathrm{T}}) + R_{\mathrm{Leq2}} + r$$
$$\dots$$
$$Z_{\mathrm{S}n} = \mathrm{j}\omega L_{\mathrm{S}n} + 1/(\mathrm{j}\omega C_{\mathrm{S}n}) + 1/(\mathrm{j}\omega C_{\mathrm{T}}) + R_{\mathrm{Leq}n} + r$$

where R_{DS} is the equivalent ON-state resistance of one MOSFET of the inverter; the switching loss of the inverter is ignored because MOSFETs can realize zero-voltage switching (ZVS) turn-ON. V_{F} is the forward voltage drop of the diode of the rectifier. $\boldsymbol{I}_{\mathrm{P}i}$ ($\boldsymbol{I}_{\mathrm{S}i}$) is the phasor of the current $I_{\mathrm{P}i}$ ($I_{\mathrm{S}i}$) carried by $L_{\mathrm{P}i}$ ($L_{\mathrm{S}i}$). $\boldsymbol{U}_{\mathrm{P0}}$ is the phasor of the first-order harmonic output voltage U_{P0} of the inverter, and it can be expressed as

$$\boldsymbol{U}_{P0} = 2\sqrt{2}U_{\mathrm{DC}} \Big/ \pi = \alpha U_{\mathrm{DC}} \tag{3}$$

where $\alpha = 2\sqrt{2}/\pi$.

III. Efficiency Optimization

A. Efficiency Analysis

The reefer containers can be considered as constant power loads, and $R_{\mathrm{Leq}i}$ changes with the output power $P_{\mathrm{Leq}i}$ consumed by the reefer container. Thus, $I_{\mathrm{S}i}$, $R_{\mathrm{Leq}i}$, $P_{\mathrm{Leq}i}$ should meet the following equation:

$$P_{\mathrm{Leq}i} = \mathbf{I}_{\mathrm{S}i} \cdot \mathbf{I}_{\mathrm{S}i}{}^{*} \cdot R_{\mathrm{Leq}i}. \tag{4}$$

The system efficiency can be expressed as

$$\eta_n = \sum_{i=1}^{n} P_{Leqi} \Bigg/ \left(\sum_{i=1}^{n} P_{Leqi} + 2\boldsymbol{I}_{P0}\boldsymbol{I}_{P0}{}^{*}R_{DS} + \sum_{i=1}^{n} A_i + \sum_{i=1}^{n} B_i \right) \tag{5}$$

where $()^{*}$ means the conjugate operation for (), $A_i = \mathrm{j}2\alpha \boldsymbol{I}_{\mathrm{S}i}V_{\mathrm{F}}$, $B_i = (\boldsymbol{I}_{\mathrm{S}i}\boldsymbol{I}_{\mathrm{S}i}{}^{*} + \boldsymbol{I}_{\mathrm{P}(i\text{-}1)}\boldsymbol{I}_{\mathrm{P}(i\text{-}1)}{}^{*})r$.

TABLE II
Parameters for the Theoretical Analysis

Symbol	Value	Symbol	Value	Symbol	Value
f	100kHz	M	104μH	r	0.19Ω
α	0.9	R_{DS}	0.1Ω	V_{F}	1.2V

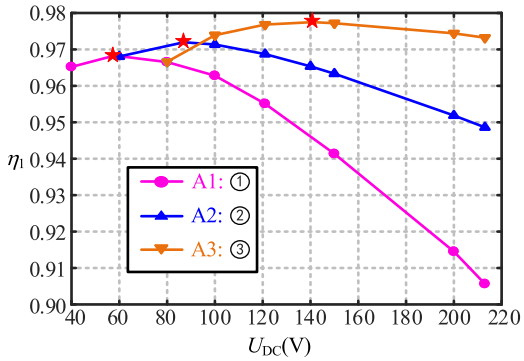

Fig. 3. η_1 against U_{DC} under various P_{Leq1}.

For a given power-relay IPT system, the parameters ω, M, r, R_{DS}, and V_{F} are given. If n is given, solving (2) and substituting (3) and (4) into (5), the system efficiency η_n can be considered as the function against U_{DC} and $P_{\mathrm{Leq1}}, \dots, P_{\mathrm{Leq}n}$

$$\eta_n = f(U_{\mathrm{DC}}, P_{Leq1}, P_{Leq2}, \dots, P_{Leqn}). \tag{6}$$

B. Maximum Efficiency

Usually, the optimal voltage $U_{\mathrm{DCopt}n}$ can be gained by solving the following equation:

$$d\eta_n / dU_{\mathrm{DC}} = 0. \tag{7}$$

It is hard to describe an analytic solution of $U_{\mathrm{DCopt}n}$ according to (7). However, it should be noted that according to the work status of containers, which are listed in Table I, there are fixed 3^n combinations of $P_{\mathrm{Leq1}}, \dots, P_{\mathrm{Leq}n}$. Thus, the numerical solutions that η_n against U_{DC} can be easily solved using the traversal algorithm in MATLAB off-line according to (6).

1) One Load Case: In the model analysis, the typical output power P_{Leq1} of a container is scaled down from 1.6/3.0/6.6 kW to 80/150/330 W, respectively. When n equals 1, with the parameters listed in Table II, the curves that η_1 against U_{DC} from 40 to 220 V is plotted in Fig. 3 under various P_{Leq1}. There is one peak point on each curve A1–A3, marked by the red pentagram, which means there exists one optimal input voltage U_{DCopt1} for maximizing efficiency. Thus, maximum efficiency can be achieved by regulating the input voltage. Serial numbers ① to ③ represent the various P_{Leq1}, which are listed in Table III. The optimal voltages U_{DCopt1} under various P_{Leq1} are also given in Table III.

2) Two Loads Case: When n equals 2, the curves that η_2 against U_{DC} from 50 to 250 V is plotted in Fig. 4. There is also one peak point marked by the red pentagram on each curve B1–B9. Thus, there exists one optimal input voltage U_{DCopt2} for maximizing efficiency under various combinations of P_{Leq1} and P_{Leq2}. Serial numbers ④ to ⑫ represent the combinations

TABLE III
INPUT-VOLTAGE-LOOKUP TABLE UNDER VARIOUS COMBINATIONS OF P_{LEQ1} AND P_{LEQ2}

S/N	$P_{\mathrm{Leq1,2}}$/W	U_{DCopt}/V	S/N	$P_{\mathrm{Leq1,2}}$/W	U_{DCopt}/V
①	80, /	58	⑦	150, 80	94
②	150, /	87	⑧	150, 150	112
③	330, /	141	⑨	150, 330	155
④	80, 80	77	⑩	330, 80	137
⑤	80, 150	98	⑪	330, 150	148
⑥	80, 330	145	⑫	330, 330	184

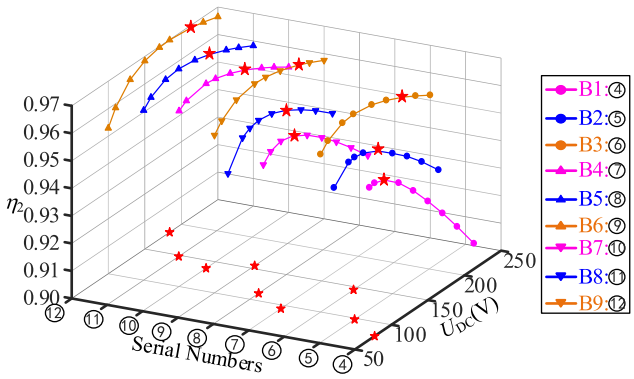

Fig. 4. η_2 against U_{DC} under various combinations of P_{Leq1} and P_{Leq2}.

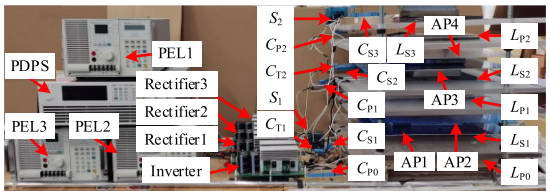

Fig. 5. Prototype of the power-relay IPT system.

of P_{Leq1} and P_{Leq2}, which are listed in Table III. The optimal voltages U_{DCopt2} under various combinations of P_{Leq1} and P_{Leq2} are given in Table III.

Generally, there is always a value of $U_{\mathrm{DCopt}n}$ to get maximum efficiency under a given combination of $P_{\mathrm{Leq1}}, \ldots, P_{\mathrm{Leq}n}$. In practice, when $P_{\mathrm{Leq1}}, \ldots, P_{\mathrm{Leq}n}$ are given, the system efficiency can be improved by regulating the input voltage according to the input-voltage-lookup table generated off-line.

IV. EXPERIMENTAL VERIFICATION

A. Prototype Setup

To verify the above analysis, a prototype of the power-relay IPT system is set up, as shown in Fig. 5. The parameters are listed in Table IV. The air gap between $L_{\mathrm{P}i}$ and $L_{\mathrm{S}(i+1)}$ is 5 cm, and the air gap between $L_{\mathrm{P}i}$ and $L_{\mathrm{P}(i+1)}$ is 20 cm. Thus, all the cross coupling can be ignored. Aluminum plates (APs) are employed to eliminate the influence of metal objects around the system.

TABLE IV
PARAMETERS OF THE POWER-RELAY IPT SYSTEM FOR THE EXPERIMENT

Symbol	Value
f	100kHz
L_{P0}, L_{P1}, L_{P2}	189.95μH, 199.85μH, 188.67μH
L_{S1}, L_{S2}, L_{S3}	193.88μH, 176.89μH, 195.33μH
C_{T1}, C_{P0}, C_{P1}, C_{P2}	24.1nF, 13.2nF, 26.1nF, 30.8nF
C_{T2}, C_{S1}, C_{S2}, C_{S3}	24.2nF, 28.0nF, 33.9nF, 12.7nF
R_{P0}, R_{P1}, R_{P2}	196mΩ, 197mΩ, 206mΩ
R_{S1}, R_{S2}, R_{S3}	189mΩ, 190mΩ, 198mΩ
M_{0_1}, M_{1_2}, M_{2_3}	104.35μH, 104.24μH, 104.37μH

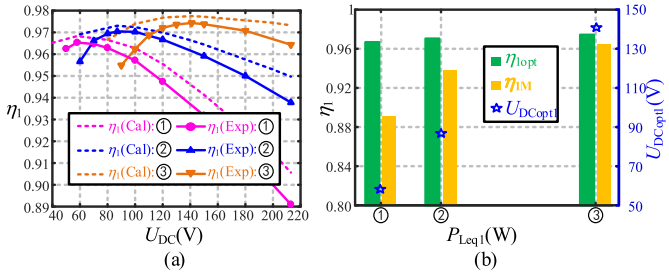

Fig. 6. η_1 against U_{DC}, and the comparison of $\eta_{1\mathrm{opt}}$ and $\eta_{1\mathrm{M}}$. (a) η_1 against U_{DC} under various P_{Leq1}. (b) Comparison of $\eta_{1\mathrm{opt}}$ and $\eta_{1\mathrm{M}}$ under various P_{Leq1}.

It should be noted that a programmable dc power supply (PDPS) and three power electronic loads (PELs) are employed in the prototype for the purpose of regulating the dc voltage.

B. Experiment Results

When n equals 1, η_1 against U_{DC} under various P_{Leq1} is illustrated in Fig. 6(a). The experimental results are consistent with the theoretical calculation results with a slight difference due to parameter tolerance. The optimal voltage can be obtained according to Table III. The comparison of the optimal system efficiency $\eta_{1\mathrm{opt}}$ and $\eta_{1\mathrm{M}}$ (when $U_{\mathrm{DC}} = U_{\mathrm{M}} = 213\,\mathrm{V}$, U_{M} is the optimal voltage under $P_{\mathrm{Leq1}} = P_{\mathrm{Leq2}} = P_{\mathrm{Leq3}} = 330\,\mathrm{W}$) under various P_{Leq1} is shown in Fig. 6(b). When $P_{\mathrm{Leq1}} = 80\,\mathrm{W}$, compared with $\eta_{1\mathrm{M}}$, $\eta_{1\mathrm{opt}}$ under $U_{\mathrm{DC}} = U_{\mathrm{DCopt1}} = 58\,\mathrm{V}$ is 96.50%, which is about 7.6% higher.

When n equals 2 and 3, the comparison of $\eta_{n\mathrm{opt}}$ and $\eta_{n\mathrm{M}}$ under various combinations of $P_{\mathrm{Leq1}}, \ldots, P_{\mathrm{Leq}n}$ are illustrated in Fig. 7. Compared with $\eta_{n\mathrm{M}}$, $\eta_{2\mathrm{opt}}$ under $U_{\mathrm{DC}} = U_{\mathrm{DCopt2}} = 77\,\mathrm{V}$ is 95.25%, which is improved by up to 7.2%, and $\eta_{3\mathrm{opt}}$ under $U_{\mathrm{DC}} = U_{\mathrm{DCopt3}} = 90\,\mathrm{V}$ is 94.29%, which is improved by up to 6.0%. Serial numbers ⑬ to ㊴ represent the combinations of P_{Leq1}, P_{Leq2}, and P_{Leq3}, which are listed in Table V.

Fig. 8(a) shows the waveform of U_{P0}, I_{P0}, U_{Re1}, and U_{Re2} when $U_{\mathrm{DC}} = 90\,\mathrm{V}$ and $P_{\mathrm{Leq1}} = P_{\mathrm{Leq2}} = P_{\mathrm{Leq3}} = 80\,\mathrm{W}$ [U_{P0} is the output voltage of the inverter, I_{P0} is the output current of the inverter, and U_{Re1} (U_{Re2}) is the input voltage of rectifiers$_1$ (rectifiers$_2$)]. The voltage of MOSFET Q_4 and the corresponding driving signal are depicted in Fig. 8(b). It is observed that ZVS turn-ON operation is achieved in the inverter. Fig. 8(c) and (d) shows the results of the power analyzer and the power losses distribution of the system, respectively. By regulating the

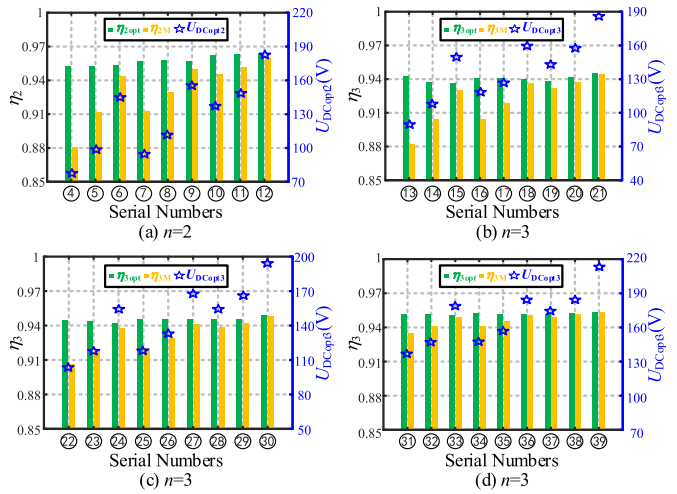

Fig. 7. Comparison of $\eta_{1\mathrm{opt}}$ and $\eta_{1\mathrm{M}}$ under various combinations of $P_{\mathrm{Leq}1},\ldots,P_{\mathrm{Leq}n}$, $n=2$, 3. (a) Combinations of $P_{\mathrm{Leq}1}$ and $P_{\mathrm{Leq}2}$: ④ to ⑫. (b) Combinations of $P_{\mathrm{Leq}1}$, $P_{\mathrm{Leq}2}$, and $P_{\mathrm{Leq}3}$: ⑬ to ㉑. (c) Combinations of $P_{\mathrm{Leq}1}$, $P_{\mathrm{Leq}2}$, and $P_{\mathrm{Leq}3}$: ㉒ to ㉚. (d) Combinations of $P_{\mathrm{Leq}1}$, $P_{\mathrm{Leq}2}$, and $P_{\mathrm{Leq}3}$: ㉛ to ㉟.

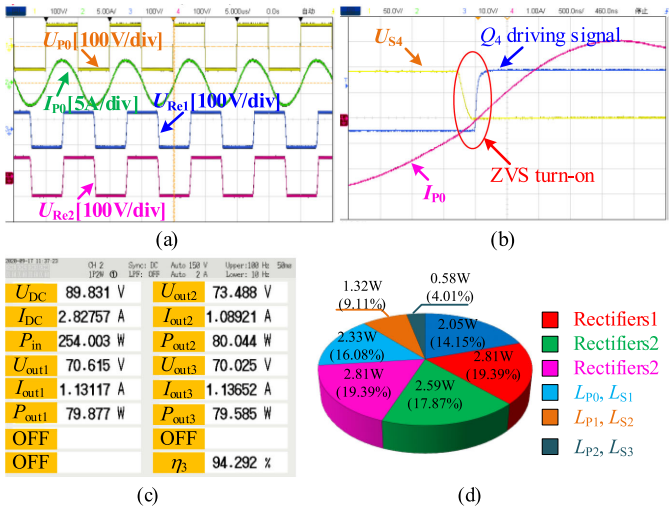

Fig. 8. Waveform and power loss distribution analysis when $U_{\mathrm{DC}}=90\,\mathrm{V}$ and $P_{\mathrm{Leq}1}=P_{\mathrm{Leq}2}=P_{\mathrm{Leq}3}=80\,\mathrm{W}$. (a) Waveform of U_{P0}, I_{P0}, U_{Re1}, and U_{Re2}. (b) Voltage of Q_4 and the corresponding driving signal. (c) Measured power and efficiency. (d) Power loss distribution of the system.

TABLE V
INPUT-VOLTAGE-LOOKUP TABLE UNDER VARIOUS COMBINATIONS OF P_{LEQ1}, P_{LEQ2}, AND P_{LEQ3}

S/N	$P_{\mathrm{Leq1,2,3}}$/× 10W	U_{DCopt}/V	*S/N*	$P_{\mathrm{Leq1,2,3}}$/× 10W	U_{DCopt}/V
⑬	8, 8, 8	90	㉗	15, 15, 33	168
⑭	8, 8, 15	109	㉘	15, 33, 8	155
⑮	8, 8, 33	150	㉙	15, 33, 15	165
⑯	8, 15, 8	110	㉚	15, 33, 33	195
⑰	8, 15, 15	127	㉛	33, 8, 8	137
⑱	8, 15, 33	158	㉜	33, 8, 15	147
⑲	8, 33, 8	143	㉝	33, 8, 33	179
⑳	8, 33, 15	158	㉞	33, 15, 8	147
㉑	8, 33, 33	186	㉟	33, 15, 15	156
㉒	15, 8, 8	103	㊱	33, 15, 33	184
㉓	15, 8, 15	117	㊲	33, 33, 8	173
㉔	15, 8, 33	155	㊳	33, 33, 15	184
㉕	15, 15, 8	118	㊴	33, 33, 33	213
㉖	15, 15, 15	133	/	/	/

input voltage according to the input-voltage-lookup table, the efficiency is greater than 94.29%.

C. Discussion

The comparison of the power-relay IPT system in [14]–[17] and that in this letter is given in Table VI. Compared with [14]–[17], efficiency optimization of the power-relay IPT system under various power distributions can be achieved, and higher efficiency can be obtained in this letter. Thus, the proposed method can save a lot of energy and is suitable for the power supply of reefer containers.

TABLE VI
COMPARISON OF THE POWER-RELAY IPT SYSTEMS IN [14]–[17] AND THIS LETTER

Proposed in	[14]	[15]	[16]	[17]	This work
Frequency	193kHz	1MHz	200kHz	200kHz	100kHz
Air gap	About 10cm	40cm	6cm	3cm	5cm
Coupling coefficient	0.04	0.035	0.24	0.49	0.55
The maximum output power	<100W	760W	30W	/	990W
The maximum efficiency	About 20%	70%	82.5%	86.6%	95.29%
Efficiency optimization	Yes	No	No	No	Yes
Power distribution of loads	Equal	Equal	Equal	Equal	Different

V. CONCLUSION

In this letter, a power-relay IPT system and the corresponding efficiency optimization method are proposed for wireless charging reefer containers. About 10.26% of precious space is saved from 212.2 to 190.4 m^2 for a fleet of containers without power towers. Besides, an experimental prototype with three loads is built to validate the proposed approach. By regulating the input voltage according to the input-voltage-lookup table, the efficiency is greater than 94.29% with an improvement by 7.6%, 7.2%, and 6.0%, compared with those without optimization (fixed input voltage 213 V) at one load (@80 W), two loads (@80 and 80 W), and three loads (@80, 80, and 80 W), respectively. The experimental results show that the proposed efficiency optimization method is valid and feasible for reefer container applications.

REFERENCES

[1] F. Lu *et al.*, "A tightly coupled inductive power transfer system for low-voltage and high-current charging of automatic guided vehicles," *IEEE Trans. Ind. Electron.*, vol. 66, no. 9, pp. 6867–6875, Sep. 2019.

[2] U. K. Madawala and D. J. Thrimawithana, "A bidirectional inductive power interface for electric vehicles in V2G systems," *IEEE Trans. Ind. Electron.*, vol. 58, no. 10, pp. 4789–4796, Oct. 2011.

[3] Y. Li *et al.*, "A new coil structure and its optimization design with constant output voltage and constant output current for electric vehicle dynamic wireless charging," *IEEE Trans. Ind. Inform.*, vol. 15, no. 9, pp. 5244–5256, Sep. 2019.

[4] W. Zhang, S. Wong, C. K. Tse, and Q. Chen, "Design for efficiency optimization and voltage controllability of series–series compensated inductive power transfer systems," *IEEE Trans. Power Electron.*, vol. 29, no. 1, pp. 191–200, Jan. 2014.

[5] W. Zhong and S. Y. Hui, "Reconfigurable wireless power transfer systems with high energy efficiency over wide load range," *IEEE Trans. Power Electron.*, vol. 33, no. 7, pp. 6379–6390, Jul. 2018.

[6] H. Li, J. Li, K. Wang, W. Chen, and X. Yang, "A maximum efficiency point tracking control scheme for wireless power transfer systems using magnetic resonant coupling," *IEEE Trans. Power Electron.*, vol. 30, no. 7, pp. 3998–4008, Jul. 2015.

[7] M. Fu, H. Yin, X. Zhu, and C. Ma, "Analysis and tracking of optimal load in wireless power transfer systems," *IEEE Trans. Power Electron.*, vol. 30, no. 7, pp. 3952–3963, Jul. 2015.

[8] M. Fu, T. Zhang, X. Zhu, P. C. Luk, and C. Ma, "Compensation of cross-coupling in multiple-receiver wireless power transfer systems," *IEEE Trans. Ind. Inform.*, vol. 12, no. 2, pp. 474–482, Apr. 2016.

[9] Y. Zhang, T. Lu, Z. Zhao, F. He, K. Chen, and L. Yuan, "Selective wireless power transfer to multiple loads using receivers of different resonant frequencies," *IEEE Trans. Power Electron.*, vol. 30, no. 11, pp. 6001–6005, Nov. 2015.

[10] Y. Kim, D. Ha, W. J. Chappell, and P. P. Irazoqui, "Selective wireless power transfer for smart power distribution in a miniature-sized multiple-receiver system," *IEEE Trans. Ind. Electron.*, vol. 63, no. 3, pp. 1853–1862, Mar. 2016.

[11] M. Fu, H. Yin, and C. Ma, "Megahertz multiple-receiver wireless power transfer systems with power flow management and maximum efficiency point tracking," *IEEE Trans. Microw. Theory Techn.*, vol. 65, no. 11, pp. 4285–4293, Nov. 2017.

[12] M. Fu, H. Yin, M. Liu, Y. Wang, and C. Ma, "A 6.78 MHz multiple-receiver wireless power transfer system with constant output voltage and optimum efficiency," *IEEE Trans. Power Electron.*, vol. 33, no. 6, pp. 5330–5340, Jun. 2018.

[13] Y. Li *et al.*, "Analysis, design, and experimental verification of a mixed high-order compensations-based WPT system with constant current outputs for driving multistring LEDs," *IEEE Trans. Ind. Electron.*, vol. 67, no. 1, pp. 203–213, Jan. 2020.

[14] Y. Zhang, T. Lu, Z. Zhao, K. Chen, F. He, and L. Yuan, "Wireless power transfer to multiple loads over various distances using relay resonators," *IEEE Microw. Wireless Compon. Lett.*, vol. 25, no. 5, pp. 337–339, May 2015.

[15] F. Lu *et al.*, "A high-efficiency and long-distance power-relay system with equal power distribution," *IEEE J. Emerg. Sel. Topics Power Electron.*, vol. 8, no. 2, pp. 1419–1427, Jun. 2020.

[16] C. Cheng, Z. Zhou, W. Li, C. Zhu, Z. Deng, and C. C. Mi, "A multi-load wireless power transfer system with series-parallel-series compensation," *IEEE Trans. Power Electron.*, vol. 34, no. 8, pp. 7126–7130, Aug. 2019.

[17] C. Cheng *et al.*, "A load-independent LCC-Compensated wireless power transfer system for multiple loads with a compact coupler design," *IEEE Trans. Ind. Electron.*, vol. 67, no. 6, pp. 4507–4515, Jun. 2020.